

How to resolve the enigma of diurnal malate remobilisation from the vacuole in plants with crassulacean acid metabolism?

Peer-reviewed author version

Ceusters, Nathalie; Borland, Anne M. & CEUSTERS, Johan (2021) How to resolve the enigma of diurnal malate remobilisation from the vacuole in plants with crassulacean acid metabolism?. In: NEW PHYTOLOGIST, 229 (6) , p. 3116 -3124.

DOI: 10.1111/nph.17070

Handle: <http://hdl.handle.net/1942/34479>

1 How to resolve the enigma of diurnal malate remobilization from the vacuole in plants with
2 crassulacean acid metabolism?

3 Nathalie Ceusters¹ (0000-0002-8374-0447) , Anne M. Borland² (0000-0003-4560-9998) , Johan
4 Ceusters^{1,3*} (0000-0002-5225-9159)

5

6 1 Faculty of Engineering Technology, Department of Biosystems, Division of Crop
7 Biotechnics, Campus Geel, KU Leuven, Kleinhoefstraat 4, 2440 Geel, Belgium.

8 2 School of Natural and Environmental Sciences, Newcastle University, Newcastle upon Tyne
9 NE1 7RU, UK.

10 3 UHasselt, Centre for Environmental Sciences, Environmental Biology, Campus Diepenbeek,
11 Agoralaan Building D, 3590 Diepenbeek, Belgium

12

13 *Corresponding author: Johan Ceusters

14 e-mail: johan.ceusters@kuleuven.be

15 telephone +3214 72 13 09

16

17 Total word count: 4344

18 Total number of figures: 2

19 Total number of tables: 3

20

21

22

23

24

25

26

27

28 **Summary**

29 Opening of stomata in plants with crassulacean acid metabolism (CAM) is mainly shifted to
30 the night period when atmospheric CO₂ is fixed by PEPC and stored as malic acid in the
31 vacuole. As such, CAM plants ameliorate transpirational water losses and display substantially
32 higher water use efficiency (WUE) compared to C₃ and C₄ plants. In the past decade significant
33 technical advances have allowed an unprecedented exploration of genomes, transcriptomes,
34 proteomes and metabolomes of CAM plants and efforts are ongoing to engineer the CAM
35 pathway in C₃ plants. Whilst research efforts have traditionally focused on nocturnal
36 carboxylation, less is known regarding the drivers behind diurnal malate remobilization from
37 the vacuole which liberates CO₂ to be fixed by Rubisco behind closed stomata. To shed more
38 light on this process, we provide a stoichiometric analysis to identify potentially rate-limiting
39 steps underpinning diurnal malate mobilization and help direct future research efforts. Within
40 this remit we address three key questions: Q1 Does light-dependent assimilation of CO₂ via
41 Rubisco dictate the rate of malate mobilization? Q2: Do the enzymes responsible for malate
42 decarboxylation limit day-time mobilization from the vacuole? Q3: Does malate efflux from
43 the vacuole set the pace of decarboxylation?

44

45 **Keywords**

46 Aluminum activated malate transporter – Crassulacean Acid Metabolism – Malate efflux –
47 Malic enzyme – PEPC – PEPCK – Rubisco – Tonoplast dicarboxylate transporter

48

49

50

51

52

53

54

55

57 **Introduction**

58 Crassulacean acid metabolism (CAM) is one of the three main metabolic pathways to
59 accommodate CO₂ fixation in the photosynthetic tissues of vascular plants. In addition to
60 tropical field crops such as pineapple and *Agave* CAM is present in a plethora of ornamentals
61 such as *Euphorbia*, *Kalanchoë*, *Yucca*, *Sansevieria*, *Sedum*, various bromeliads, orchids and
62 cacti. In contrast to C₃ and C₄ plants, CAM plants predominantly fix atmospheric CO₂ at night
63 when evapotranspiration rates are low, enabling plants to close stomata for much of the day and
64 thereby optimising water-use efficiency (WUE). This important water-conserving trait has
65 fostered diverse recent efforts to determine the minimal requirements for engineering the CAM
66 pathway into non-CAM crops (CAM Biodesign) in order to improve WUE whilst maintaining
67 high productivity (Borland *et al.*, 2014; Lim *et al.*, 2019). The diel cycle of CAM photosynthesis
68 is commonly divided into four phases that integrate patterns of net CO₂ uptake and changes in
69 the abundance of key metabolites that define carbon supply and demand over the 24 h cycle
70 (Osmond, 1978). When stomata are open at night during Phase I, external CO₂ is converted to
71 HCO₃⁻ and then sequestered via phosphoenolpyruvate carboxylase (PEPC) using the 3-carbon
72 substrate phosphoenolpyruvate (PEP), which is provided from the glycolytic breakdown of
73 carbohydrate accumulated during the previous day (Fig. 1). The final 4-C product, malate, is
74 then pumped in the vacuole, following an inside positive electrical potential difference across
75 the tonoplast generated by a dedicated V-ATPase. During the subsequent light period (Phase
76 III), malate is released from the vacuole and decarboxylated in the cytosol by either malic
77 enzyme (ME) or a combination of malate dehydrogenase (MDH) and PEPcarboxykinase
78 (PEPCK), releasing CO₂ inside the mesophyll cells. Subsequently, CO₂ is refixed by ribulose-
79 1,5-bisphosphate carboxylase-oxygenase (Rubisco) behind closed stomata (Borland *et al.*,
80 2011). These major CAM phases are punctuated by Phase II at the start of the day and Phase
81 IV at the end of the day (Borland & Taybi, 2004), with open stomata allowing fixation of
82 atmospheric CO₂ by either PEPC and/or Rubisco. The four CAM phases typically show a high
83 degree of plasticity in terms of magnitude and duration, which appears to be critical for
84 optimizing carbon gain and water use under a changing environment (Ceusters *et al.*, 2009,
85 2010, 2011).

86 Temporal coordination and co-regulation of both carboxylating enzymes, i.e. PEPC and
87 Rubisco, brings about a unique and flexible carboxylation capacity in CAM plants over the diel
88 cycle (Fig. 1). Circadian and metabolic control of nocturnal carboxylation is mediated via

89 reversible phosphorylation of PEPC and is well documented. PEPC is activated at night via
90 phosphorylation of a serine residue near the N-terminus of the protein which renders the enzyme
91 more sensitive to PEP and the positive effectors, glucose-6-P and triose-P and less sensitive to
92 the allosteric inhibitor, malate (Hartwell *et al.*, 1999; Borland *et al.*, 1999; Nimmo, 2000). As
93 a first step towards installing CAM into C₃ plants, Kebeish *et al.* (2012) used dark-induced
94 promoters to control the nocturnal overexpression of a PEPC engineered with reduced malate
95 sensitivity in stably transformed Arabidopsis. Whilst these transformed Arabidopsis plants
96 showed enhanced stomatal opening and transpiration rates at night (Kebeish *et al.*, 2012), a key
97 challenge for CAM engineering will be achieving coordinated activation–deactivation of PEPC
98 with Rubisco and malate decarboxylation over the diel cycle.

99 In contrast to the nocturnal (night-time) carboxylation process, much less is known
100 about the diurnal (day-time) biochemical events in CAM plants and one process in particular,
101 the daytime translocation of malate out of the vacuole, has received relatively little attention to
102 date. Light intensity seems to be a critical factor in orchestrating diurnal malate metabolism and
103 different potential rate limiting steps have been suggested: i) efflux from the vacuole; ii)
104 liberation of CO₂ in the cytosol by decarboxylation or iii) assimilation of the liberated CO₂ via
105 Rubisco in the chloroplast (Luttge, 2004). Driven by its growing eco-agricultural importance,
106 the field of CAM research is now advancing quickly and important technical breakthroughs in
107 the past decade have allowed an unprecedented exploration of CAM genomes, transcriptomes,
108 proteomes and metabolomes (Ming *et al.*, 2015; Yang *et al.*, 2017; Ceusters *et al.*, 2019;
109 Abraham *et al.*, 2020). In combination with rapidly progressing computational modelling
110 approaches (Shameer *et al.*, 2018; Chomthong & Griffiths, 2020) a variety of new tools and
111 genetic resources are now available to shed more light on diurnal malate metabolism in CAM
112 plants. In this research review three important key questions are addressed: Q1 Does light-
113 dependent assimilation of CO₂ via Rubisco dictate the rate of malate mobilization? Q2: Do the
114 enzymes responsible for malate decarboxylation limit day-time mobilization from the vacuole?
115 Q3: Does malate efflux from the vacuole set the pace of decarboxylation? Answers are provided
116 by considering detailed stoichiometric analyses based on the available literature and important
117 directions for future research efforts are highlighted and discussed.

118

119 **Q1: Does light-dependent assimilation of CO₂ via Rubisco dictate the rate of malate**
120 **mobilization?**

121 Factors influencing the light-dependent assimilation of CO₂ via Rubisco and its
122 relationship to the onset and subsequent rate of malate mobilization during the photoperiod in
123 CAM plants are still not fully resolved. Rubisco activity in CAM plants appears to be tightly
124 regulated during the light period but differs from C₃ plants in terms of a more protracted
125 activation that is independent of light intensity (Maxwell *et al.*, 1999, 2002; Griffiths *et al.*,
126 2008). In situations where PEPC activity extends beyond the night period for several hours into
127 the photoperiod, Rubisco in CAM plants remains inactive as indicated by low rates of electron
128 transport and increased non-photochemical quenching which curtails the capacity for light use
129 and dissipation being exceeded (Griffiths *et al.*, 2008). Rubisco activation requires the
130 reversible binding of activator CO₂ and a light-dependent non-enzymatic modification called
131 carbamylation which is stabilized by binding of Mg²⁺ (Lorimer & Miziorko, 1980; Portis,
132 1992). The stromal enzyme Rubisco activase (RCA) is critically important for mediating the
133 activation and maintenance of Rubisco activity and operates by removing inhibitory sugar
134 phosphates from the catalytic site of Rubisco (Parry *et al.*, 2008). The slow and protracted
135 activation of Rubisco during the day in CAM species appears to be regulated, at least in part,
136 by transcriptional regulation of RCA, which shows an increase in protein abundance as the
137 photoperiod progresses that is independent of light intensity (Maxwell *et al.*, 2002). A low
138 activation status for Rubisco at the start of the photoperiod in CAM plants is predicted to curtail
139 competition between the carboxylases. Davies & Griffiths (2012) demonstrated that this low
140 Rubisco activation state at the start of the photoperiod, was maintained under free running
141 conditions of constant light and temperature in CAM-performing *Mesembryanthemum*
142 *crystallinum* and coincided with the initiation of malate breakdown and stomatal closure at each
143 subjective dawn. Such observations pose the hypothesis that Rubisco activation status in CAM
144 species is mediated by an interplay of circadian and metabolic cues which might include
145 [malate] and/or pCO₂ (Borland & Taybi, 2004; Davies & Griffiths, 2012).

146 The elevated [CO₂] that is generated from day-time decarboxylation behind closed
147 stomata has suggested pCO₂ as a key signal for coordinating the rate of CO₂ consumption by
148 Rubisco with malic acid remobilisation from the vacuole during Phase III of CAM (Maxwell
149 *et al.*, 1999; Lüttge, 2002; Borland & Taybi, 2004). During Phase III, pCO₂ can range between
150 0.08 and 2.50 % in the leaf air spaces which generally exceeds substrate saturation of Rubisco
151 which is estimated around 0.2-0.4% (Maxwell *et al.*, 1998; Lüttge, 2002). Malate
152 decarboxylation is commonly marked by high, non-saturated rates of electron transport, with
153 Rubisco activity, RCA abundance and activation state increasing as Phase III progresses and

154 malate content diminishes. Quantitative comparisons of measured Rubisco activities (uptake of
155 CO₂) and degradation rates of malate (liberation of CO₂) in the leaf mesophyll cells during
156 Phase III would tend to refute the hypothesis that Rubisco assimilation might represent a
157 possible bottleneck in malate remobilization (Table 1). Furthermore, enhancement of Rubisco
158 activity throughout Phase III points to a feed-forward upregulation of Rubisco activation/RCA
159 in response to the declining pCO₂ as malate content is exhausted (Maxwell *et al.*, 1998).

160 Sensing of pCO₂ during the shift from Phase III to Phase IV is also indicated at a
161 metabolic level by further increases in the abundance of RCA and activation state of Rubisco
162 towards the end of the photoperiod when cytosolic malate is exhausted and pCO₂ may drop as
163 low as 0.01% (Maxwell *et al.*, 1998). This further enhancement of Rubisco activity in Phase IV
164 occurs at a time when stomata have reopened and diffusional limitations to drawdown of
165 atmospheric CO₂ imposed by closely packed succulent cells in CAM tissues is most likely to
166 limit photon utilization. Clearly, the day-time mobilization of malate from the vacuole and its
167 subsequent decarboxylation alter the catalytic context for Rubisco and RCA in CAM plants by
168 generating a metabolic ‘feast and famine’ of internal [CO₂] supply (Maxwell *et al.*, 2002;
169 Griffiths *et al.*, 2008). Recent studies have begun to investigate structure/function relationships
170 for both Rubisco and RCA in CAM lineages (Shivhare & Mueller-Cajar, 2017; Hermida-
171 Carrera *et al.*, 2020). Such approaches promise new insights on the molecular evolution of these
172 proteins and their catalytic optimization for the dynamic changes in pCO₂ that are generated
173 as a consequence of the onset and cessation of malate mobilisation during the daytime phases
174 of CAM. Further work is required to establish if the engineering of CAM into C3 plants will
175 require a modification to the kinetic properties of Rubisco and/or its activase in order to
176 optimize diurnal malate mobilization.

177 **Q2: Do the enzymes responsible for malate decarboxylation limit day-time mobilization**
178 **from the vacuole?**

179 Decarboxylation of malate can proceed either via NAD(P)-Malic enzyme (ME) or
180 phosphoenolpyruvate carboxykinase (PEPCK) dependent on the species considered (Fig. 1).
181 The relative contributions of mitochondrial NAD-ME and chloroplastic/cytosolic NADP-ME
182 to malate decarboxylation in the light have been debated for many years. In 1976, Ditttrich
183 postulated that NAD-ME was not the dominating decarboxylase in Crassulaceae, but rather an
184 additional support to NADP-ME activity. However, Dever *et al.* (2015) used transgenic RNAi
185 lines of the obligate CAM species *Kalanchoë fedtschenkoi* to demonstrate that NAD-ME is the
186 key decarboxylase, with a minor contribution from NADP-ME. Subsequent analyses of the

187 transcriptome (Yang *et al.*, 2017) and proteome (Abraham *et al.*, 2020) of *K. fedtschenkoi*
188 identified diel changes in transcript and protein abundance of *kfNAD* ME1. Protein abundance
189 of *kfNAD* ME1 peaked in the middle of the photoperiod at a time when the rate of malate
190 decarboxylation is maximal, suggesting a level of transcriptional regulation over the daytime
191 breakdown of malate via ME (Abraham *et al.*, 2020). ME liberates CO₂ from malate to
192 accommodate further refixation by Rubisco in the mesophyll via the Calvin-Benson cycle (Fig.
193 1). The byproduct of this reaction, pyruvate, is consequently converted to PEP at the expense
194 of ATP by cytosolic/plastidic pyruvate orthophosphate dikinase (PPDK) and metabolized and
195 stored during the day either as chloroplastic starch or vacuolar sugars dependent on the species
196 considered (Holtum *et al.*, 2005). PPDK is essential for CAM activity as demonstrated by RNAi
197 knockdown in *K. fedtschenkoi* although the RNAi lines also showed a 30 % decrease in
198 extractable NAD-ME activity relative to wild type (Dever *et al.*, 2015). Furthermore, low PPDK
199 activity was noted in rNAD-ME lines of *K. fedtschenkoi* and was attributed to inactivation of
200 PPDK by phosphorylation in the transgenic plants (Dever *et al.*, 2015). These data indicate
201 post-translational control over malate decarboxylation that is subject to metabolic regulation by
202 CAM-associated metabolites, possibly malate. Diel changes in phosphopeptide abundance of
203 PPDK protein in *K. fedtschenkoi* were reported by Abraham *et al.* (2020) and are consistent
204 with phosphorylation/inactivation of PPDK during the night in this CAM species.
205 Phosphorylation of PPDK in C₄ plants is catalyzed by PPDK regulatory protein (PPDK-RP;
206 Chastain *et al.*, 2011). An ortholog of PPDK-RP in *K. fedtschenkoi* showed increased protein
207 abundance at the end of the photoperiod and for most of the dark period which would be
208 consistent with inactivation of PPDK when malate is accumulating in the vacuole, rather than
209 being processed via decarboxylation (Abraham *et al.*, 2020). Moreover, in the inducible CAM
210 plant *M. crystallinum* PPDK-RP transcript abundance was upregulated when switching to CAM
211 mode (Lim *et al.*, 2019). Further research is required to understand if PPDK and its regulatory
212 protein play pivotal roles in the temporal coordination of decarboxylation with malate efflux
213 from the vacuole during the photoperiod in CAM plants.

214 PEPCK serves as an oxaloacetate (OAA) decarboxylase and requires the prior operation
215 of malate dehydrogenase (MDH) to convert malate into OAA. With extractable activities 4-110
216 times higher compared to measured PEPCK activities in a range of CAM plants (Dittrich *et al.*,
217 1973), MDH is unlikely to impose a limit on the rate of diurnal malate degradation. Also the
218 intrinsic PEPCK activity itself does not seem to be a plausible candidate for restraining diurnal
219 malate mobilization from the vacuole. In 2014 Ceusters *et al.* reported a consistent delay in

220 organic acid breakdown in the CAM bromeliad *A. 'Maya'*, which occurred ~ 4 and 12 h into
221 the photoperiod under either low fluence red or green light in comparison to low fluence blue
222 light. However, no changes in PEPCK (main decarboxylating enzyme in this bromeliad)
223 activity were noticed, indicating that this delay in malate mobilization could not be attributed
224 to insufficient intrinsic decarboxylating capacity but rather to curtailed efflux of malate from
225 the vacuole. These light quality experiments also stress the need to further our understanding
226 of the interaction of different photoreceptors such as phytochromes, cryptochromes and
227 phototropins regarding the temporal coordination of the malic acid cycle in CAM plants. Since
228 PEPCK mediated OAA decarboxylation immediately yields CO₂ and PEP, no additional PDK
229 activity is needed and only low activity of the latter have indeed been measured in different
230 PEPCK types of CAM plants (Black *et al.*, 1996). Plant PEPCK is cytosolic, as is PEPC, so a
231 reciprocal regulation of both activities is predicted for effective operation of the CAM cycle
232 and to avoid futile cycling of ATP and CO₂. Native PEPCK is phosphorylated in some C₄ leaves
233 and in all CAM leaves studied to date (Walker & Leegood, 1996; Walker *et al.*, 1997). It is
234 hypothesised that phosphorylation might occur at night, rendering the enzyme less active,
235 although a connection between the phosphorylation status of PEPCK and a decreased activity
236 in darkened leaves has only been demonstrated for the enzyme from the C₄ plant Guinea grass
237 (Walker *et al.*, 2002). The kinetic properties of PEPCK in the CAM plant *A. comosus* are subject
238 to modulation by pH and metabolites that include malate, citrate and succinate (Martín *et al.*,
239 2011), so allosteric regulation of PEPCK-mediated decarboxylation could potentially offer a
240 further layer of control over diel malate mobilization in CAM.

241 To further investigate whether malate or OAA decarboxylation represent a potential rate
242 limiting processes that could impact malate efflux from the vacuole, we provide a
243 stoichiometric comparison of reported, intrinsic activities of the decarboxylating (related)
244 enzymes with malic acid processing in a range of different CAM species (Table 2). Plants
245 relying on PEPCK mediated decarboxylation such as *Aechmea 'Maya'*, *A. comosus*, *Clusia*
246 *rosea* and *Hoya carnosa* clearly display extractable activities far in excess of those needed to
247 accommodate the observed malate degradation. Values of extractable *in vitro* ME activities in
248 the CAM plants *K. daigremontiana*, *K. pinnata* and *Vanilla planifolia* are more in line with the
249 observed rates of malate breakdown but still seem to have sufficiently high capacity to avoid a
250 rate limiting effect under normal conditions of homeostasis. *In vivo*, however, it is likely that
251 decarboxylating enzyme activity will be modified by cellular conditions such as pH and energy
252 charge and/or by reversible phosphorylation/dephosphorylation. A further literature review of

253 published values for PPK activities in different CAM plants show comparable values to those
254 of ME and hence do not seem to confer a rate limiting step in diurnal malate metabolism either
255 (Table 3).

256

257 **Q3: Does Malate efflux from the vacuole set the pace of decarboxylation?**

258 Malate efflux from the vacuole is still one of the least understood processes in CAM
259 research and different mechanisms of tonoplast transport have been proposed for diurnal malate
260 remobilization. These include passive diffusion, a proton-linked symporter and/or a dedicated
261 malate anion channel (Fig. 2) (Smith *et al.*, 1996). In its undissociated form, $\text{H}_2\text{malate}^0$ can
262 indeed passively diffuse out of the vacuole but considering the relatively low pK_a of ~ 3.40 , this
263 process is proposed to be relevant only at the lowest vacuolar pH around dawn (Lüttge & Smith,
264 1984). During the major part of the light period, vacuolar efflux occurs predominantly as
265 Hmalate^- and/or malate^{2-} and a wealth of evidence gathered in the preceding decades indicates
266 an intimate stoichiometry of $2 \text{H}^+ : \text{malate}^{2-}$ (or alternatively $1 \text{H}^+ : \text{Hmalate}^-$). In addition, a
267 recent integrated diel flux balance analysis (FBA) study by Shameer *et al.* (2018) integrating
268 cytosolic, vacuolar, chloroplastic, peroxisomal and mitochondrial metabolism in a realistic
269 CAM model, also predicts a considerable export of protons out of the vacuole during daytime
270 malate remobilization. These considerations suggest a close relationship between proton and
271 malate efflux out of the vacuole during the major part of Phase III.

272 Based on investigations in the C_3 model species *Arabidopsis thaliana* the tonoplast
273 dicarboxylate transporter (tDT) has been postulated as a plausible candidate to accommodate
274 diurnal malate remobilization in CAM plants (Emmerlich *et al.*, 2003; Holtum *et al.*, 2005;
275 Borland *et al.*, 2009). More recent work in the CAM species pineapple also showed significant
276 diel cycling of tDT transcripts with peak abundance noted around dawn (Wai *et al.*, 2017).
277 Whilst the exact transport properties of tDT have proved rather elusive, a more recent study by
278 Frei *et al.* (2018) confirmed a specific preference for dianion substrates such as malate,
279 fumarate, citrate and succinate but not α -ketoglutarate, gluconate, sulphate or phosphate. As
280 other related members of the solute carrier family 13 (SLC13) transporters had previously been
281 characterized as sodium carboxylate symporters, it is tempting to propose the existence of tDT
282 mediated co-transport of mal^{2-} and 2H^+ . This would provide both an explanation for
283 concomitant remobilization of malate ions and protons out of the vacuole (Holtum *et al.*, 2005).
284 However, detailed proteoliposome studies by Frei *et al.* (2018) indicated tDT as acting in an

285 electroneutral manner by employing an antiport mechanism exchanging diverse dicarboxylates
286 such as citrate and malate.

287 Another potential candidate for accommodating vacuolar malate efflux during the light
288 period is the aluminum activated malate transporter (ALMT). Originally revealed in studies
289 investigating aluminum toxicity, these anion channels have been found to play significant roles
290 in diverse physiological processes such as avoidance of metal toxicity, mineral nutrition, ion
291 balances, turgor regulation, fruit quality and guard cell functioning (Sharma *et al.*, 2016).
292 Originally ALMT's were associated with nocturnal malate accumulation in CAM since initial
293 patch clamp analyses in *K. daigremontiana* were indicative of an inward-rectifying anion-
294 selective channel which imposes unidirectional transport of malate from the cytosol to the
295 vacuole (Hafke *et al.*, 2003). Also in grapes, *VvALMT9* has been found to be constitutively
296 expressed in the mesocarp tissue of berries with a significant upregulation during fruit
297 maturation when malic and tartaric acid accumulate in the vacuoles (De Angeli *et al.*, 2013).
298 However detailed patch clamp experiments by Meyer *et al.* (2011) showed for the first time
299 that *AtALMT6* could function either as a malate influx or efflux channel depending on the
300 tonoplast potential, cytosolic malate concentration and the vacuolar pH. Moreover, the
301 particular switch between influx and efflux can occur at physiological membrane potentials,
302 thereby favoring malate export out of the vacuole when vacuolar pH has dropped. Based on
303 these outcomes it can be questioned whether a similar principle could account for both the
304 nocturnal sequestration of malate in the vacuole, which is accommodated by significant
305 acidification and its diurnal remobilization after a certain pH threshold has been exceeded.
306 Recent studies focusing on transcriptional changes over the diel course also seem to highlight
307 a specific role for ALMT concerning CAM functioning (Wai & VanBuren, 2018; Ferrari *et al.*,
308 2020). These considerations reopen the debate as to whether the malate influx channel in CAM
309 plants can indeed be gated in order to act as an efflux channel at the start of the photoperiod.
310 This interesting hypothesis has already been postulated by Smith *et al.* (1996) but at that time
311 it was believed that the malate channel was strictly inward-rectified thereby only permitting
312 vacuolar malate influx (Iwasaki *et al.*, 1992).

313 Irrespective of the exact nature of the putative malate transporter, strict coupling is
314 required between the diurnal export of malate and its associated protons out of the vacuole on
315 one hand and the decarboxylation events and cytosolic proton metabolism on the other. Whilst
316 the decarboxylation reactions themselves have been well characterized, the biochemical nature
317 of the most important diurnal proton consuming reactions in the cytosol is still obscure. Recent

318 FBA CAM models highlight a putative key role for the mitochondrial P_i/H^+ symporter (PiC) to
319 relieve the cytosol from its diurnal “proton pressure” and thus curtail over-acidification
320 (Shameer *et al.*, 2018). In *Arabidopsis* different isoforms of PiC have been characterized with
321 high abundance in the mitochondrial membrane as predominant carriers to replenish the matrix
322 with inorganic phosphate in order to secure ATP synthesis (Millar & Heazlewood, 2003).
323 Transporters in CAM mitochondria have received much less scrutiny but mitochondrial
324 adenylate and dicarboxylate transporters, belonging to the same mitochondrial carrier protein
325 superfamily (mCP) as PiC, have already been identified in the inducible common ice plant,
326 namely McANT2 and McDCT2 respectively (Kore-eda *et al.*, 2005). Further work in this area
327 is highly encouraged to shed more light on how CAM plants secure cytosolic proton
328 homeostasis during the diurnal period of malate degradation. Due to its relatively small volume,
329 the cytosol is especially prone to over-acidification. In 2011 Ceusters *et al.* showed that a
330 substantial reduction in light availability (from ~ 3 to $0.5 \text{ mol photons m}^{-2} \text{ d}^{-1}$) during the
331 photoperiod resulted in chlorenchyma cell death after 8 hours. These observations that specific
332 environmental conditions can bring about uncoupling between malate efflux and its further
333 processing, support our proposed view that the efflux process itself is likely to be dictated by
334 an integration of circadian and metabolic signals which would provide a basis for the
335 synchronization and plasticity of metabolism that is inherent to CAM

336

337 **Conclusions and future perspectives**

338 Among others, early pioneers in CAM research such as Barry Osmond and Ulrich Lüttge
339 already questioned the enigma of diurnal malate remobilization from the vacuole in CAM plants
340 some decades ago (Osmond, 1978; Lüttge, 2000, 2002).

341 In the past decade significant technical advances have allowed an unprecedented
342 exploration of CAM genomes, transcriptomes, proteomes and metabolomes (Ming *et al.*, 2015;
343 Yang *et al.*, 2017; Ceusters *et al.*, 2019). Successful implementation of the RNAi approach in
344 the CAM model species *Kalanchoë* by the research group of James Hartwell has provided an
345 experimental means to further unravel the roles of specific enzymes and putative transporters
346 (Dever *et al.*, 2015; Boxall *et al.*, 2020). More recently, John Cushman and colleagues have
347 engineered *Arabidopsis* to over-express several proteins from *M. crystallinum* that
348 accommodate CAM carboxylating and decarboxylating events. Their work showed that malate
349 contents and stomatal conductance patterns indeed can be altered (Lim *et al.*, 2019). However,

350 several important challenges related to CAM Biodesign (i.e. transfer of the CAM
351 photosynthetic pathway into C₃ or C₄ plants) still need to be addressed. These include
352 mechanisms for achieving appropriate transport, storage and degradation of carbohydrate to
353 fuel PEPC mediated carboxylation as well as appropriate coordination between the diel
354 carboxylation processes. Whilst nocturnal CO₂ fixation (Phase I) is solely mediated by PEPC,
355 the diurnal carboxylation processes are much more complex.

356 Recently, rapid progress in the advances of implementing CRISPR/Cas9 in CAM plants
357 (Liu *et al.*, 2019), have opened up a novel toolbox to accommodate functional genomics
358 research. However, in order to avoid getting overwhelmed by a plethora of ‘omics’ data,
359 computational modelling approaches are also becoming increasingly important (Chomthong &
360 Griffiths, 2020). These models are typically based on a bottom up approach and do not require
361 information of the complete transcription-gene regulatory network to provide realistic
362 simulations of plant metabolism (Owen & Griffiths, 2013; Cheung *et al.*, 2014). In 2018
363 Shameer *et al.* published a two phase CAM model accounting for the diurnal and nocturnal
364 phases and integrating cytosolic, chloroplastic, mitochondrial and peroxisomal metabolism.
365 Efforts are underway to develop a more detailed diel model based on a 2h basis that will capture
366 the dynamics of the four phases of CAM and provide an unprecedented level of detail, including
367 the diurnal remobilization of malate.

368 In conclusion we postulate that the vacuolar efflux of malate itself might be a key
369 candidate for orchestrating the onset and duration/rate of diurnal deacidification in leaves of
370 CAM plants. Controlled release of malate from the vacuole which is influenced by both
371 environmental and circadian cues also offers a mechanistic explanation for the observed
372 plasticity in the magnitude and duration of the daytime Phases. During the early morning Phase
373 II stomates open and malate degradation needs to be curtailed to avoid futile cycling of carbon.
374 Net CO₂ uptake in Phase II can, in some circumstances, occur for several hours dependent on
375 environmental conditions or the species considered (Ceusters *et al.*, 2009, 2010). When malate
376 degradation is initiated due to its controlled release from the vacuole Phase II shifts towards
377 Phase III which is characterized by high intracellular pCO₂ and stomatal closure. Finally, when
378 malate efflux comes to an end, its decarboxylation will slow down, intracellular pCO₂ will drop
379 and stomates will reopen to accommodate direct atmospheric CO₂ uptake in Phase IV.
380 However, more important questions still need to be resolved in the near-future to further unravel
381 the exact interplay of environmental and circadian control on diurnal malate and H⁺
382 remobilization from the vacuole. These include:

- 383 • What is the exact identity of the diurnal malate transporter(s)?
384 • How does vacuolar H⁺ efflux occur during daytime?
385 • What is the contribution of mitochondrial transporters and metabolism to secure diurnal
386 cytosolic proton homeostasis?
387 • What is the exact role of the different photoreceptors such as phytochromes,
388 cryptochromes and phototropins in mediating environmental control over diurnal efflux
389 of malate?

390

391 **Acknowledgements**

392 The authors would like to thank Internal Funds KU Leuven for financial support.

393

References

- 394 **Abraham PE, Castano NH, Cowan-Turner D, Barnes J, Poudel S, Hettich R, Flütsch S, Santelia D,**
395 **Borland AM. 2020.** Peeling back the layers of crassulacean acid metabolism: functional
396 differentiation between *Kalanchoë fedtschenkoi* epidermis and mesophyll proteomes. *The Plant*
397 *Journal* **103**: 869–888.
- 398 **Arata H, Iwasaki I, Kusumi K, Nishimura M. 1992.** Thermodynamics of Malate Transport across the
399 Tonoplast of Leaf Cells of CAM Plants. *Plant and Cell Physiology* **33**: 873–880.
- 400 **Black CC, Chen J-Q, Doong RL, Angelov MN, Sung SJS. 1996.** Alternative Carbohydrate Reserves Used
401 in the Daily Cycle of Crassulacean Acid Metabolism. In: Winter K, Smith JAC, eds. Ecological Studies.
402 Crassulacean Acid Metabolism: Biochemistry, Ecophysiology and Evolution. Berlin, Heidelberg:
403 Springer, 31–45.
- 404 **Borland AM, Griffiths H. 1997.** A comparative study on the regulation of C₃ and C₄ carboxylation
405 processes in the constitutive crassulacean acid metabolism (CAM) plant *Kalanchoë daigremontiana*
406 and the C₃-CAM intermediate *Clusia minor*. *Planta* **201**: 368–378.
- 407 **Borland AM, Griffiths H, Hartwell J, Smith JAC. 2009.** Exploiting the potential of plants with
408 crassulacean acid metabolism for bioenergy production on marginal lands. *Journal of Experimental*
409 *Botany* **60**: 2879–2896.
- 410 **Borland AM, Hartwell J, Jenkins GI, Wilkins MB, Nimmo HG. 1999.** Metabolite Control Overrides
411 Circadian Regulation of Phosphoenolpyruvate Carboxylase Kinase and CO₂ Fixation in Crassulacean
412 Acid Metabolism. *Plant Physiology* **121**: 889–896.
- 413 **Borland AM, Hartwell J, Weston DJ, Schlauch KA, Tschaplinski TJ, Tuskan GA, Yang X, Cushman JC.**
414 **2014.** Engineering crassulacean acid metabolism to improve water-use efficiency. *Trends in Plant*
415 *Science* **19**: 327–338.

- 416 **Borland AM, Taybi T. 2004.** Synchronization of metabolic processes in plants with Crassulacean acid
417 metabolism. *Journal of Experimental Botany* **55**: 1255–1265.
- 418 **Borland AM, Técsi LI, Leegood RC, Walker RP. 1998.** Inducibility of crassulacean acid metabolism
419 (CAM) in *Clusia* species; physiological/biochemical characterisation and intercellular localization of
420 carboxylation and decarboxylation processes in three species which exhibit different degrees of
421 CAM. *Planta* **205**: 342–351.
- 422 **Borland AM, Zambrano VAB, Ceusters J, Shorrocks K. 2011.** The photosynthetic plasticity of
423 crassulacean acid metabolism: an evolutionary innovation for sustainable productivity in a changing
424 world. *New Phytologist* **191**: 619–633.
- 425 **Boxall SF, Kadu N, Dever LV, Kneřová J, Waller JL, Gould PJD, Hartwell J. 2020.** *Kalanchoë* PPC1 Is
426 Essential for Crassulacean Acid Metabolism and the Regulation of Core Circadian Clock and Guard
427 Cell Signaling Genes. *The Plant Cell* **32**: 1136–1160.
- 428 **Brilhaus D, Bräutigam A, Mettler-Altmann T, Winter K, Weber APM. 2016.** Reversible Burst of
429 Transcriptional Changes during Induction of Crassulacean Acid Metabolism in *Talinum triangulare*.
430 *Plant Physiology* **170**: 102–122.
- 431 **Ceusters J, Borland AM, Ceusters N, Verdoodt V, Godts C, De Proft MP. 2010.** Seasonal influences
432 on carbohydrate metabolism in the CAM bromeliad *Aechmea* ‘Maya’: consequences for
433 carbohydrate partitioning and growth. *Annals of Botany* **105**: 301–309.
- 434 **Ceusters J, Borland AM, Godts C, Londers E, Croonenborghs S, Van Goethem D, De Proft MP. 2011.**
435 Crassulacean acid metabolism under severe light limitation: a matter of plasticity in the shadows?
436 *Journal of Experimental Botany* **62**: 283–291.
- 437 **Ceusters J, Borland AM, Londers E, Verdoodt V, Godts C, De Proft MP. 2008.** Diel Shifts in
438 Carboxylation Pathway and Metabolite Dynamics in the CAM Bromeliad *Aechmea* ‘Maya’ in
439 Response to Elevated CO₂. *Annals of Botany* **102**: 389–397.
- 440 **Ceusters J, Borland AM, Londers E, Verdoodt V, Godts C, Proft MPD. 2009.** Differential usage of
441 storage carbohydrates in the CAM bromeliad *Aechmea* ‘Maya’ during acclimation to drought and
442 recovery from dehydration. *Physiologia Plantarum* **135**: 174–184.
- 443 **Ceusters J, Borland AM, Taybi T, Frans M, Godts C, De Proft MP. 2014.** Light quality modulates
444 metabolic synchronization over the diel phases of crassulacean acid metabolism. *Journal of*
445 *Experimental Botany* **65**: 3705–3714.
- 446 **Ceusters N, Luca S, Feil R, Claes JE, Lunn JE, Van den Ende W, Ceusters J. 2019.** Hierarchical
447 clustering reveals unique features in the diel dynamics of metabolites in the CAM orchid
448 *Phalaenopsis*. *Journal of Experimental Botany* **70**: 3269–3281.
- 449 **Chastain CJ, Failing CJ, Manandhar L, Zimmerman MA, Lakner MM, Nguyen THT. 2011.** Functional
450 evolution of C4 pyruvate, orthophosphate dikinase. *Journal of Experimental Botany* **62**: 3083–3091.
- 451 **Cheung CYM, Poolman MG, Fell DA, Ratcliffe RG, Sweetlove LJ. 2014.** A Diel Flux Balance Model
452 Captures Interactions between Light and Dark Metabolism during Day-Night Cycles in C3 and
453 Crassulacean Acid Metabolism Leaves. *Plant Physiology* **165**: 917–929.
- 454 **Chomthong M, Griffiths H. 2020.** Model approaches to advance crassulacean acid metabolism
455 system integration. *The Plant Journal* **101**: 951–963.

456 **Christopher JT, Holtum J. 1996.** Patterns of Carbon Partitioning in Leaves of Crassulacean Acid
457 Metabolism Species during Deacidification. *Plant Physiology* **112**: 393–399.

458 **Davies BN, Griffiths H. 2012.** Competing carboxylases: circadian and metabolic regulation of Rubisco
459 in C3 and CAM *Mesembryanthemum crystallinum* L. *Plant, Cell & Environment* **35**: 1211–1220.

460 **De Angeli A, Zhang J, Meyer S, Martinoia E. 2013.** AtALMT9 is a malate-activated vacuolar chloride
461 channel required for stomatal opening in Arabidopsis. *Nature Communications* **4**: 1804.

462 **Dever LV, Boxall SF, Kneřová J, Hartwell J. 2015.** Transgenic Perturbation of the Decarboxylation
463 Phase of Crassulacean Acid Metabolism Alters Physiology and Metabolism But Has Only a Small Effect
464 on Growth. *Plant Physiology* **167**: 44–59.

465 **Dittrich P. 1976.** Nicotinamide Adenine Dinucleotide-specific “Malic” Enzyme in *Kalanchoë*
466 *daigremontiana* and Other Plants Exhibiting Crassulacean Acid Metabolism. *Plant Physiology* **57**:
467 310–314.

468 **Dittrich P, Campbell WH, Black CC. 1973.** Phosphoenolpyruvate Carboxykinase in Plants Exhibiting
469 Crassulacean Acid Metabolism. *Plant Physiology* **52**: 357–361.

470 **Emmerlich V, Linka N, Reinhold T, Hurth MA, Traub M, Martinoia E, Neuhaus HE. 2003.** The plant
471 homolog to the human sodium/dicarboxylic cotransporter is the vacuolar malate carrier. *Proceedings*
472 *of the National Academy of Sciences* **100**: 11122–11126.

473 **Ferrari RC, Bittencourt PP, Rodrigues MA, Moreno-Villena JJ, Alves FRR, Gastaldi VD, Boxall SF,**
474 **Dever LV, Demarco D, Andrade SCS, et al. 2020.** C4 and crassulacean acid metabolism within a single
475 leaf: deciphering key components behind a rare photosynthetic adaptation. *New Phytologist* **225**:
476 1699–1714.

477 **Frei B, Eisenach C, Martinoia E, Hussein S, Chen X-Z, Arrivault S, Neuhaus HE. 2018.** Purification and
478 functional characterization of the vacuolar malate transporter tDT from Arabidopsis. *Journal of*
479 *Biological Chemistry* **293**: 4180–4190.

480 **González-Olmedo JL, Fundora Z, Molina LA, Abdulnour J, Desjardins Y, Escalona M. 2005.** New
481 contributions to propagation of pineapple (*Ananas comosus* L. Merr) in temporary immersion
482 bioreactors. *In Vitro Cellular & Developmental Biology - Plant* **41**: 87–90.

483 **Griffiths H, Robe WE, Girnus J, Maxwell K. 2008.** Leaf succulence determines the interplay between
484 carboxylase systems and light use during Crassulacean acid metabolism in *Kalanchoë* species. *Journal*
485 *of Experimental Botany* **59**: 1851–1861.

486 **Hafke JB, Hafke Y, Smith JAC, Lüttge U, Thiel G. 2003.** Vacuolar malate uptake is mediated by an
487 anion-selective inward rectifier. *The Plant Journal* **35**: 116–128.

488 **Hartwell J, Gill A, Nimmo GA, Wilkins MB, Jenkins GI, Nimmo HG. 1999.** Phosphoenolpyruvate
489 carboxylase kinase is a novel protein kinase regulated at the level of expression. *The Plant Journal* **20**:
490 333–342.

491 **Hermida-Carrera C, Fares MA, Font-Carrascosa M, Kapralov MV, Koch MA, Mir A, Molins A, Ribas-**
492 **Carbó M, Rocha J, Galmés J. 2020.** Exploring molecular evolution of Rubisco in C3 and CAM
493 Orchidaceae and Bromeliaceae. *BMC Evolutionary Biology* **20**: 11.

- 494 **Holtum JAM, Smith JAC, Neuhaus HE. 2005.** Intracellular transport and pathways of carbon flow in
495 plants with crassulacean acid metabolism. *Functional Plant Biology* **32**: 429–449.
- 496 **Iwasaki I, Arata H, Kijima H, Nishimura M. 1992.** Two Types of Channels Involved in the Malate Ion
497 Transport across the Tonoplast of a Crassulacean Acid Metabolism Plant. *Plant Physiology* **98**: 1494–
498 1497.
- 499 **Jaiswal S, Sawhney S. 2006.** Correlation of epiphyllous bud differentiation with foliar senescence in
500 crassulacean succulent *Kalanchoe pinnata* as revealed by thidiazuron and ethrel application. *Journal*
501 *of Plant Physiology* **163**: 717–722.
- 502 **Kebeish R, Niessen M, Oksaksin M, Blume C, Peterhaensel C. 2012.** Constitutive and dark-induced
503 expression of *Solanum tuberosum* phosphoenolpyruvate carboxylase enhances stomatal opening
504 and photosynthetic performance of *Arabidopsis thaliana*. *Biotechnology and Bioengineering* **109**:
505 536–544.
- 506 **Kondo A, Nose A, Yuasa H, Ueno O. 2000.** Species variation in the intracellular localization of
507 pyruvate, Pi dikinase in leaves of crassulacean-acid-metabolism plants: an immunogold electron-
508 microscope study. *Planta* **210**: 611–621.
- 509 **Kore-eda S, Noake C, Ohishi M, Ohnishi J, Cushman JC. 2005.** Transcriptional profiles of organellar
510 metabolite transporters during induction of crassulacean acid metabolism in *Mesembryanthemum*
511 *crystallinum*. *Functional Plant Biology* **32**: 451–466.
- 512 **Lim SD, Lee S, Choi W-G, Yim WC, Cushman JC. 2019.** Laying the Foundation for Crassulacean Acid
513 Metabolism (CAM) Biodesign: Expression of the C4 Metabolism Cycle Genes of CAM in *Arabidopsis*.
514 *Frontiers in Plant Science* **10**.
- 515 **Liu D, Chen M, Mendoza B, Cheng H, Hu R, Li L, Trinh CT, Tuskan GA, Yang X. 2019.** CRISPR/Cas9-
516 mediated targeted mutagenesis for functional genomics research of crassulacean acid metabolism
517 plants. *Journal of Experimental Botany* **70**: 6621–6629.
- 518 **Lorimer GH, Mizioroko HM. 1980.** Carbamate formation on the .epsilon.-amino group of a lysyl
519 residue as the basis for the activation of ribulosebiphosphate carboxylase by carbon dioxide and
520 magnesium(2+). *Biochemistry* **19**: 5321–5328.
- 521 **Lüttge U. 2000.** The tonoplast functioning as the master switch for circadian regulation of
522 crassulacean acid metabolism. *Planta* **211**: 761–769.
- 523 **Lüttge U. 2002.** CO₂-concentrating: consequences in crassulacean acid metabolism. *Journal of*
524 *Experimental Botany* **53**: 2131–2142.
- 525 **Lüttge U. 2004.** Ecophysiology of Crassulacean Acid Metabolism (CAM). *Annals of Botany* **93**: 629–
526 652.
- 527 **Lüttge U, Smith JAC. 1984.** Mechanism of passive malic-acid efflux from vacuoles of the CAM
528 plant *Kalanchoë daigremontiana*. *The Journal of Membrane Biology* **81**: 149–158.
- 529 **Martin CE, Hsu RC-C, Lin T-C. 2010.** Sun/shade adaptations of the photosynthetic apparatus of *Hoya*
530 *carnosa*, an epiphytic CAM vine, in a subtropical rain forest in northeastern Taiwan. *Acta Physiologiae*
531 *Plantarum* **32**: 575–581.

532 **Martín M, Rius SP, Podestá FE. 2011.** Two phosphoenolpyruvate carboxykinases coexist in the
533 Crassulacean Acid Metabolism plant *Ananas comosus*. Isolation and characterization of the smaller
534 65kDa form. *Plant Physiology and Biochemistry* **49**: 646–653.

535 **Maxwell K, Badger MR, Osmond CB. 1998.** A comparison of CO₂ and O₂ exchange patterns and the
536 relationship with chlorophyll fluorescence during photosynthesis in C₃ and CAM plants. *Functional*
537 *Plant Biology* **25**: 45–52.

538 **Maxwell K, Borland AM, Haslam RP, Helliker BR, Roberts A, Griffiths H. 1999.** Modulation of Rubisco
539 Activity during the Diurnal Phases of the Crassulacean Acid Metabolism Plant
540 *Kalanchoëdaigremontiana*. *Plant Physiology* **121**: 849–856.

541 **Maxwell K, Griffiths H, Helliker B, Roberts A, Haslam RP, Girnus J, Robe WE, Borland AM. 2002.**
542 Regulation of Rubisco activity in crassulacean acid metabolism plants: better late than never.
543 *Functional Plant Biology* **29**: 689–696.

544 **Meyer S, Scholz-Starke J, Angeli AD, Kovermann P, Burla B, Gambale F, Martinoia E. 2011.** Malate
545 transport by the vacuolar AtALMT6 channel in guard cells is subject to multiple regulation. *The Plant*
546 *Journal* **67**: 247–257.

547 **Millar AH, Heazlewood JL. 2003.** Genomic and Proteomic Analysis of Mitochondrial Carrier Proteins
548 in *Arabidopsis*. *Plant Physiology* **131**: 443–453.

549 **Ming R, VanBuren R, Wai CM, Tang H, Schatz MC, Bowers JE, Lyons E, Wang M-L, Chen J, Biggers E,**
550 **et al. 2015.** The pineapple genome and the evolution of CAM photosynthesis. *Nature Genetics* **47**:
551 1435–1442.

552 **Nimmo HG. 2000.** The regulation of phosphoenolpyruvate carboxylase in CAM plants. *Trends in Plant*
553 *Science* **5**: 75–80.

554 **Osmond CB. 1978.** Crassulacean Acid Metabolism: A Curiosity in Context. *Annual Review of Plant*
555 *Physiology* **29**: 379–414.

556 **Owen NA, Griffiths H. 2013.** A system dynamics model integrating physiology and biochemical
557 regulation predicts extent of crassulacean acid metabolism (CAM) phases. *New Phytologist* **200**:
558 1116–1131.

559 **Parry MAJ, Keys AJ, Madgwick PJ, Carmo-Silva AE, Andralojc PJ. 2008.** Rubisco regulation: a role for
560 inhibitors. *Journal of Experimental Botany* **59**: 1569–1580.

561 **Portis AR. 1992.** Regulation of Ribulose 1,5-Bisphosphate Carboxylase/Oxygenase Activity. *Annual*
562 *Review of Plant Physiology and Plant Molecular Biology* **43**: 415–437.

563 **Puthur J. 2005.** Influence of light intensity on growth and crop productivity of *Vanilla Planifolia* Andr.
564 *General and Applied Plant Physiology* **31**: 215–224.

565 **Shameer S, Baghalian K, Cheung CYM, Ratcliffe RG, Sweetlove LJ. 2018.** Computational analysis of
566 the productivity potential of CAM. *Nature Plants* **4**: 165–171.

567 **Sharma T, Dreyer I, Kochian L, Piñeros MA. 2016.** The ALMT Family of Organic Acid Transporters in
568 Plants and Their Involvement in Detoxification and Nutrient Security. *Frontiers in Plant Science* **7**:
569 1488.

- 570 **Shivhare D, Mueller-Cajar O. 2017.** In Vitro Characterization of Thermostable CAM Rubisco Activase
571 Reveals a Rubisco Interacting Surface Loop. *Plant Physiology* **174**: 1505–1516.
- 572 **Smith JAC, Ingram J, Tsiantis MS, Barkla BJ, Bartholomew DM, Bettey M, Pantoja O, Pennington AJ.**
573 **1996.** Transport Across the Vacuolar Membrane in CAM Plants. In: Winter K, Smith JAC, eds.
574 Ecological Studies. Crassulacean Acid Metabolism: Biochemistry, Ecophysiology and Evolution. Berlin,
575 Heidelberg: Springer, 53–71.
- 576 **Szymańska R, Kruk J. 2008.** Tocopherol content and isomers' composition in selected plant species.
577 *Plant Physiology and Biochemistry* **46**: 29–33.
- 578 **Wai CM, VanBuren R. 2018.** Circadian Regulation of Pineapple CAM Photosynthesis. In: Ming R, ed.
579 Plant Genetics and Genomics: Crops and Models. Genetics and Genomics of Pineapple. Cham:
580 Springer International Publishing, 247–258.
- 581 **Wai CM, VanBuren R, Zhang J, Huang L, Miao W, Edger PP, Yim WC, Priest HD, Meyers BC, Mockler**
582 **T, et al. 2017.** Temporal and spatial transcriptomic and microRNA dynamics of CAM photosynthesis
583 in pineapple. *The Plant Journal* **92**: 19–30.
- 584 **Walker RP, Acheson RM, Técsi LI, Leegood RC. 1997.** Phosphoenolpyruvate Carboxykinase in C4
585 Plants: Its Role and Regulation. *Functional Plant Biology* **24**: 459–468.
- 586 **Walker RP, Chen Z-H, Acheson RM, Leegood RC. 2002.** Effects of Phosphorylation on
587 Phosphoenolpyruvate Carboxykinase from the C4 Plant Guinea Grass. *Plant Physiology* **128**: 165–172.
- 588 **Walker RP, Leegood RC. 1996.** Phosphorylation of phosphoenolpyruvate carboxykinase in plants.
589 Studies in plants with C4 photosynthesis and Crassulacean acid metabolism and in germinating seeds.
590 *Biochemical Journal* **317**: 653–658.
- 591 **Yang X, Hu R, Yin H, Jenkins J, Shu S, Tang H, Liu D, Weighill DA, Cheol Yim W, Ha J, et al. 2017.** The
592 Kalanchoë genome provides insights into convergent evolution and building blocks of crassulacean
593 acid metabolism. *Nature Communications* **8**: 1899.

Table 1

Comparison of published values for Rubisco activity (expressed as the amount of incorporated CO₂) with calculated, diurnal malic acid degradation rates in two CAM species. For *Clusia* values are expressed in $\mu\text{mol gFW}^{-1} \text{h}^{-1}$ and for *Kalanchoë* values are expressed in $\text{mmol m}^{-2} \text{h}^{-1}$.

Plant Species	Malic Acid degradation	Rubisco	References
<i>Clusia rosea</i>	14.0	42	(Borland <i>et al.</i> , 1998)
<i>Kalanchoë daigremontiana</i>	12.0	72 – 101	(Maxwell <i>et al.</i> , 1999)
	8.64	11 – 16	(Borland & Griffiths, 1997)

Table 2

Comparison of reported, intrinsic activities of the different types of decarboxylating enzymes (ME or PEPCK) with calculated, diurnal malic acid degradation rates, in a range of different CAM plants.

Plant Species	Malic Acid degradation ($\mu\text{mol gFW}^{-1} \text{h}^{-1}$)	NAD(P)-ME ($\mu\text{mol CO}_2 \text{gFW}^{-1} \text{h}^{-1}$)	PEPCK ($\mu\text{mol CO}_2 \text{gFW}^{-1} \text{h}^{-1}$)	References
<i>Aechmea</i> 'Maya'	3.3	/	33 ± 4	(Ceusters <i>et al.</i> , 2014)
<i>Ananas comosus</i>	3.5	6.12 ± 1	151 ± 29	(Christopher & Holtum, 1996) (González-Olmedo <i>et al.</i> , 2005)
<i>Clusia rosea</i>	14.0	trace amounts	240	(Borland <i>et al.</i> , 1998)
<i>Hoya carnosa</i>	5.7	25 ± 2	126 ± 36	(Christopher & Holtum, 1996) (Martin <i>et al.</i> , 2010)
<i>Kalanchoë daigremontiana</i>	6	17 ± 5	ND	(Christopher & Holtum, 1996) (Szymańska & Kruk, 2008)
<i>Kalanchoë pinnata</i>	8.3	20 ± 8	ND	(Christopher & Holtum, 1996) (Jaiswal & Sawhney, 2006)
<i>Vanilla planifolia</i>	5.4	70 ± 17	ND	(Christopher & Holtum, 1996) (Puthur, 2005)

Data of enzymatic activities are means ± standard deviation.

ME – malic enzyme; PEPCK – PEPcarboxykinase; ND – Non detectable

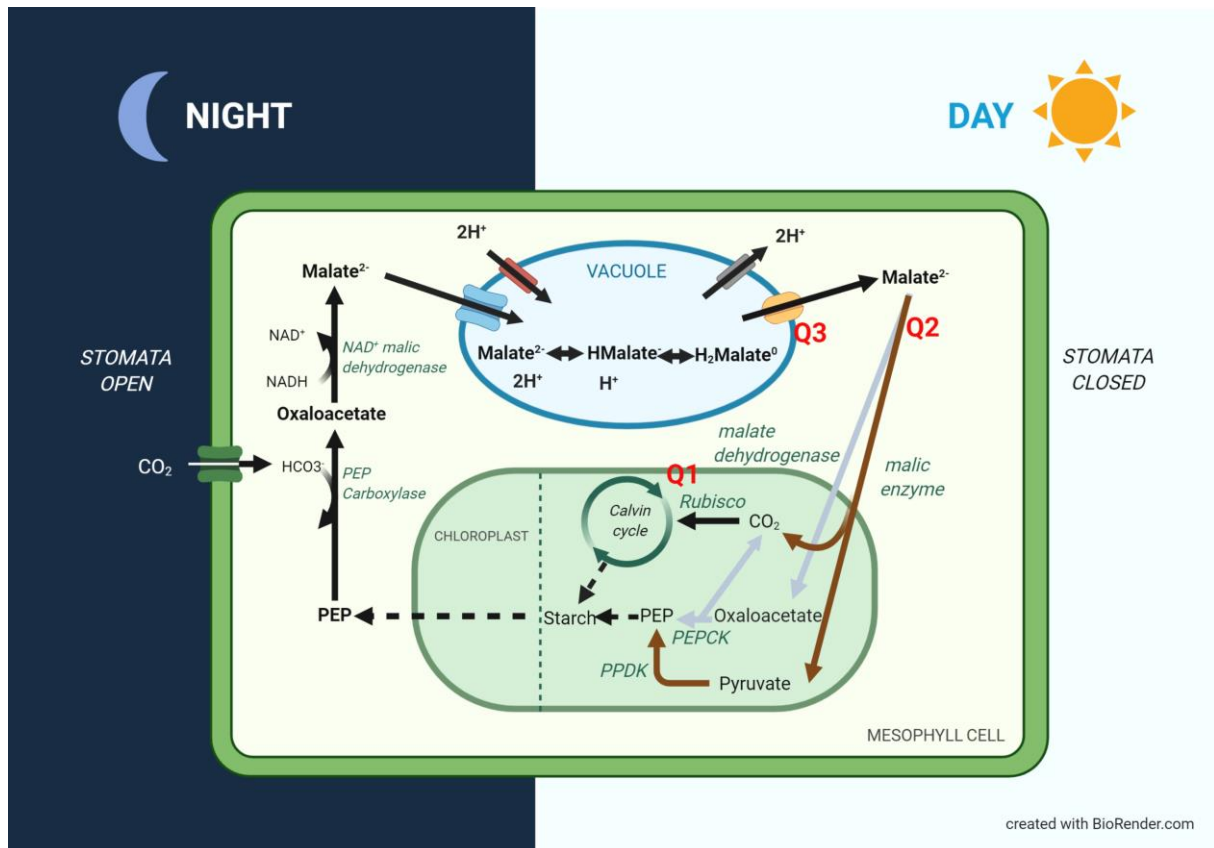
Table 3

Comparison of published values of intrinsic enzyme activity for pyruvate orthophosphate dikinase (PPDK) and NAD(P)-malic enzyme (ME) in different CAM taxa.

Taxa	PPDK	NAD(P)-ME
	$\mu\text{mol mg}^{-1} \text{Chl}^{-1} \text{h}^{-1}$	
Agavaceae	40 -50	43 - 785
Aizoaceae	19	16 - 195
Cactaceae	8 - 200	5 - 920
Crassulaceae	5 - 240	16 - 385
Dracaenaceae	6 - 70	19 - 127

Values based on Black *et al.* (1996) and Kondo *et al.* (2000).

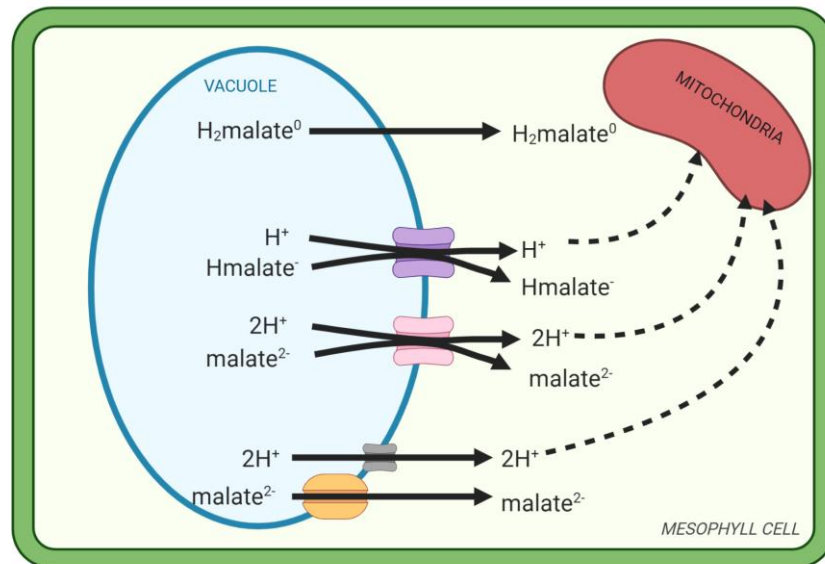
Figure 1



Simplified representation of crassulacean acid metabolism with emphasis on malate metabolism. Dotted arrows represent multiple steps and different species of malate can exist in the vacuole dependent on the pH, i.e. H₂malate⁰, Hmalate⁻ and malate²⁻. The mechanism of malate efflux will be discussed in more detail in Figure 2. Three important key questions are addressed in this review i.e. Q1: Does light-dependent assimilation of CO₂ via Rubisco dictate malate mobilization from the vacuole? Q2: Is malate decarboxylation limiting its vacuolar mobilization? Dependent on the species considered, decarboxylation of malate can proceed either via malic enzyme and PPK (gray arrows) or via malate dehydrogenase and PEPCK (brown arrows). Q3: Does malate efflux set the pace for diurnal malate metabolism?

PEP – phosphoenolpyruvate; PPK - cytosolic/plastidic pyruvate orthophosphate dikinase; PEPCK – PEPcarboxykinase

Figure 2



created with BioRender.com

Representation of different hypotheses regarding diurnal malate and proton movements in crassulacean acid metabolism plants namely: passive diffusion of $H_2malate^0$; proton linked symport of $Hmalate^-$ and $malate^{2-}$; and a dedicated malate anion channel for $malate^{2-}$. Whilst $H_2malate^0$ transport is only considered to be meaningful only at the very lowest pH (around dawn) experimental evidence strongly suggests concomitant transport of malate anions (i.e. either $Hmalate^-$ or $malate^{2-}$) and protons out of the vacuole. A putative $H^+/Hmalate^-$ or $2H^+/malate^{2-}$ co-transporter has not yet been identified whilst dedicated malate anion channels have already been characterized such as ALMT and tDT. Recent flux balance analysis models indicate that considerable amounts of protons are consumed by the mitochondria to secure cytosolic proton homeostasis (indicated by dotted arrows).